ACCOUNTS of chemical research

Article

Cite This: Acc. Chem. Res. 2019, 52, 1428−1438

pubs.acs.org/accounts

A Twist on Nonlinear Optics: Understanding the Unique Response of π-Twisted Chromophores

Alexander J.-T. Lou and Tobin J. Marks*

Department of Chemistry and the Materials Research Center, Northwestern University, 2145 Sheridan Road, Evanston, Illinois 60208, United States

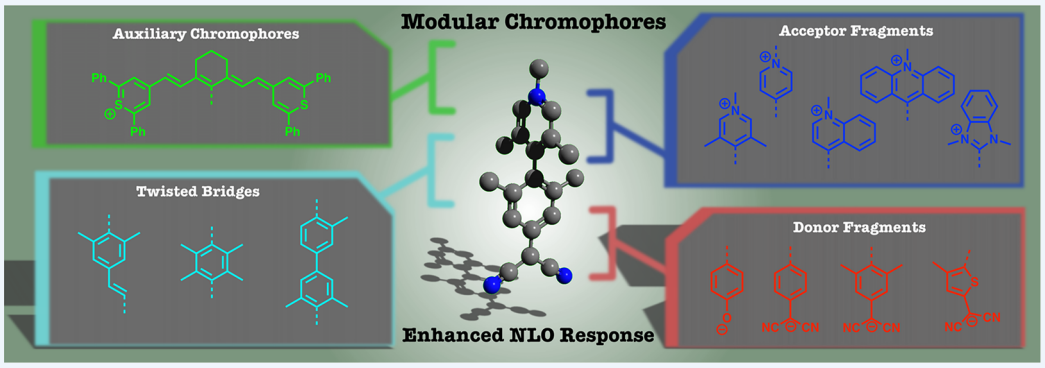

CONSPECTUS: Materials with large nonlinear optical (NLO) response have the ability to manipulate the frequency and phase of incident light and exhibit phenomena that form the basis of modern telecommunication systems. In molecule-based materials, the second- and third-order NLO performance is related to the hyperpolarizability (β) and second hyperpolarizability (γ) of the constituent molecules. The search for higher β materials is driven by the desire to keep pace with expanding demand for high speed data transmission, while discovery of high γ chromophores is crucial for the development of emergent photonic technologies reliant on manipulation of "light-with-light". For decades, it was believed that for highest performance, organic NLO materials must be composed of planar π-system chromophores, and much exploratory research focused on subtle molecular modifications, which generally yielded incremental increases in $\mu\beta$, where μ is the molecular dipole moment. The surprising recent discovery that twisted π-system chromophores can exhibit dramatically higher β values than their planar analogues has revealed a new design paradigm and stimulated the development of high performance twisted intramolecular charge transfer (TICT) chromophores, which are composed of electron-donating and electron-accepting π-substituents joined by a sterically constrained twisted biaryl fragment. In such chromophores, the twisting of the π-system enforces charge separation in the electronic ground state, leading to large dipole moments and low-lying charge-transfer excitations. This unique electronic structure forms the basis for enhanced NLO response, with an archetypal TICT chromophore, **TMC-2**, exhibiting very large second- ($\mu\beta = 24\,000 \times 10^{-48}$ esu) and third-order ($\gamma = 1.4 \times 10^{-33}$ esu) metrics in dilute low-polarity solutions. This Account summarizes several approaches to enhance $\mu\beta$ in various environments, including (1) manipulating the biaryl torsional angle, (2) modifying the electron accepting fragment, (3) extending conjugation, (4) adding multiple twisted fragments, (5) modifying chromophore side chains, and (6) tuning the chromophore environment. Another set of modifications is explored to enhance γ, including (1) coupling to a cyanine dye to hybridize the cyanine and TICT orbitals, (2) manipulating the donor and acceptor group identity. The extensive modifications described above yield a detailed understanding of TICT chromophore molecular NLO response and unambiguous evidence that such chromophores have the potential to revolutionize organic electro-optics.

1. INTRODUCTION

Twisting of π-conjugated systems is an important factor that dictates electronic and physical properties relevant to many fields and applications. For example, torsion can influence device morphology and mobilities in organic photovoltaic materials[1] and is a key parameter affecting thermally activated delayed fluorescence in molecules used for OLEDs.[2,3] Torsion can also be imparted by electronic excitation; some donor-π-acceptor chromophores may access a *twisted intramolecular charge transfer* (TICT) state, in which twisting of the π-system leads to decoupling of the donor and acceptor moieties.[4,5] The molecules reported here represent a unique subset of TICT chromophores; the incorporation of steric constraints and aromatic stabilization causes a reordering of the energy levels, resulting in a highly charge-separated TICT ground state.[6]

In this Account, we discuss the nonlinear optical (NLO) response of TICT chromophores. Second-order NLO-active chromophores constitute the active component in electro-optic (E-O) materials, which are critical for many modern

Received: February 13, 2019
Published: April 30, 2019

DOI: 10.1021/acs.accounts.9b00077
Acc. Chem. Res. 2019, 52, 1428−1438

telecommunication, computing, and sensing applications.[7,8] It is now well established that the bulk E-O response of organic materials can exceed that of conventional inorganic E-O crystals by a factor of several hundred, thus motivating significant interest in this field.[9] In materials that incorporate E-O active chromophores into host polymer matrices, the bulk E-O response depends primarily on the molecular first hyperpolarizability (β), the molecular dipole moment (μ), as well as the number density (N) and orientation of the chromophores within the matrix.[9] While conventional approaches, such as bond-length alternation (BLA) and the careful tailoring of donor/acceptor groups, have led to significant increases in $\mu\beta$,[9] the nonclassical TICT chromophores described here exhibit some of the highest $\mu\beta$ values reported to date and are therefore promising constituents for next-generation E-O materials.[10] Specific details on incorporating such chromophores into bulk E-O materials are beyond the scope of this Account, and we refer the reader to refs 7, 8, 11, and 12. The third-order NLO response of TICT chromophores is also promising; large γ values are accompanied by low linear and nonlinear loss, making TICT chromophores excellent candidates for applications that require manipulation of light with light, such as all-optical switching.[13−15] This Account summarizes experimental studies focused on understanding the impact of molecular structure modification on the electronic structure and NLO properties of these systems, with the ultimate goal of realizing high-performance materials for E-O and photonic devices.

2. TICT GEOMETRIC AND ELECTRONIC STRUCTURE

The TICT chromophores discussed here are composed of (1) a cationic acceptor fragment, (2) an anionic donor fragment, and (3) a biaryl bridge that is twisted as a result of synthetically introduced steric repulsion between bulky substituents (Figure 1A). The electronic ground state is defined by the relative contributions of the zwitterionic/aromatic (ZA) and neutral/quinoidal (NQ) resonance forms (Figure 1C), which can be assessed by spectroscopic and crystallographic techniques.[10,16−20] The crystallographically derived biaryl distance, labeled (ring)C−C(ring) in Figure 1B, indicates whether the biaryl bond is more typical of a C−C or C═C bond and, consequently, if the structure is best represented by the ZA or NQ resonance structure (Table 1).

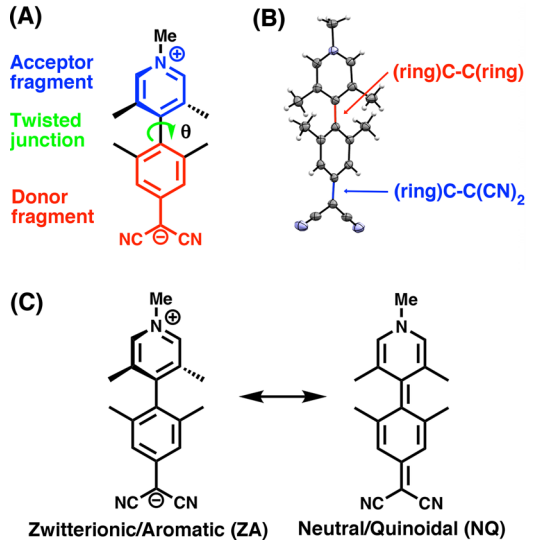

Figure 1. (A) Typical TICT chromophore with a sterically enforced biaryl torsional angle, θ. (B) ORTEP image of the molecular structure (30% ellipsoids) of **TMC-1** indicating the key C−C bond distances.[16] (C) Zwitterionic/aromatic and neutral/quinoidal resonance contributions to ground-state electronic structure.

Table 1. TICT Chromophore Crystallographic Parameters: Torsional Angle (θ) and Key C−C Bond Distances[16,18−20]

structure	torsional angle (θ)	(ring)C−C(ring) (Å)	(ring)C−C(CN)$_2$ (Å)
TM-1[16]	87	1.489(2)	
TMC-2[16]	90	1.488(5)	1.463(5)
FMC[20]	9	1.449(6)	1.429(6)
2TTMC[19]	78	1.486(7)	1.454(6)
2TTMC-a[19]	85	1.482(4)	1.452(4)
3TTMC[19]	86	1.483(6)	1.471(4)
4TTMC[19]	88	1.421(6)	1.448(6)
B0TMC-2[18]	70	1.465(4)	1.445(4)
B1TMC-2[18]	89	1.474(8)	1.438(8)
B2TMC-2[18]	79	1.478(4)	1.450(4)

For TICT chromophores, this distance is between 1.497(4) and 1.421(6) Å, which has greater similarity to a bimesityl C−C (1.505 Å) than to a typical quinoidal C═C bond (~1.349 Å).[10,16−20] The (ring)C−C(CN)$_2$ distance can also indicate aromatic character; these distances are between 1.438(8) and 1.463(5) Å, which is significantly longer than a typical (ring)C═C(CN)$_2$ bond length of ~1.392 Å.[10,16−20] Thus, the ground state structure is dominated by the ZA form, partially as a result of aromatic stabilization of the donor and acceptor group, which lowers the energy of the ZA form even in moderately twisted structures.[20] Additionally, the steric constraints which enforce the biaryl torsion serve to limit the overlap of bridging carbon p orbitals, thereby reducing the NQ contribution as $\theta \rightarrow 90°$. Vibrational spectroscopic evidence supports the correlation of ZA/NQ character with θ; in highly twisted structures, characteristic dicyanomethanide stretching frequencies indicate that the donor groups support nearly full negative charges, and linear optical absorbance spectra reveal larger solvatochromic shifts with increased θ, which reflects an enhanced ground state dipole moment consistent with the ZA resonance form.[10,16−20]

2.1. Linear Optical Absorbance

Singly twisted TICT chromophores exhibit a low-lying interfragment charge transfer transition (ICT) in the region of λ_{ICT} = 400−700 nm, as well as higher energy subfragment (SF) excitations (Figure 2A). In general, the identity of the donor and acceptor groups dictate λ_{ICT}, while the torsional angle (θ) of the biaryl bridge is related to the ICT strength. TICT chromophores tend to exhibit negative solvatochromic behavior, meaning that the ground state is significantly more stabilized than the ICT state in polar solvents, leading to blue-shifting of λ_{ICT} (Figure 2B). This is a result of large ground state dipole moments (μ_g), ranging from 20−80 D; the excited state dipole moments of the ICT states (μ_e) are very small in comparison.[19]

DOI: 10.1021/acs.accounts.9b00077
Acc. Chem. Res. 2019, 52, 1428−1438

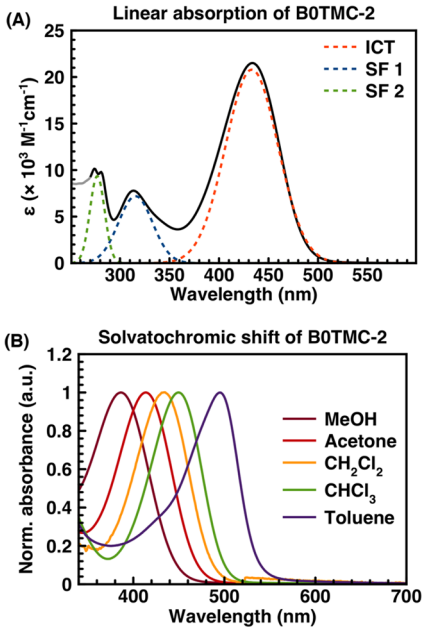

Figure 2. Linear absorption spectra of a typical TICT chromophore, **B0TMC-2**. (A) Absorption of **B0TMC-2** in DCM; dotted lines model the charge transfer (ICT) and subfragment (SF) transitions. (B) Solvatochromic shift of the ICT transition of **B0TMC-2** in solvents of varying polarity. Reproduced with permission from ref 18. Copyright 2018 American Chemical Society.

3. SECOND-ORDER NONLINEAR OPTICAL RESPONSE (β)

The pursuit of organic chromophores having large hyperpolarizabilities, β, has spanned several decades, and although numerous different and elegant approaches have led to marked enhancements in NLO response,[9,11,21] none have produced a greater jump in nonlinearity than TICT chromophores.[16] In addition to excellent β values, TICT chromophores exhibit high thermal stability (T_d < 300 C) and wide optical transparency windows (λ_{max} < 700 nm), both of which have proven to be elusive chromophore properties in the existing literature. Furthermore, TICT chromophores are some of the only known substances to exceed the apparent limit ($\beta_{int} = 10^{-3/2}$) on intrinsic hyperpolarizability, β_{int}, which is defined as the ratio of the measured β value to the theoretical maximum β for a molecule with a given excitation energy and number of electrons.[22] This observation is consistent with the recent finding that "modulated conjugation" or "phase disruption" can greatly enhance β_{int} in model quantum systems.[23,24]

3.1. Theoretical Foundations of Large NLO Response

The origin of the large β in TICT chromophores can be understood using the combination of a chemically intuitive two-site Hückel model and the commonly used two-state equation for β (eq 1).[25] Here

$$\beta = \frac{{\mu_{eg}}^2 \Delta\mu_{eg}}{{E_{eg}}^2} \quad (1)$$

β is defined by the transition moment (μ_{eg}), the change in state dipole moment ($\Delta\mu_{eg}$), and the difference in energy (E_{eg}) between the ground and first electronic excited state. The two-site Hückel approach represents the acceptor (φ_a) and donor subunit (φ_d) as separate wave functions, such that one can express the quantities in eq 1 in terms of the difference in subunit energy (V), the molecular dipole moment (μ), and resonance integral (t), which relates to the electronic connectivity of the donor and acceptor subunits. To incorporate the effects of molecular torsion, t is approximated as $t = \cos(\theta)$.[25−27]

This Hückel model shows that as θ approaches 90°, $\Delta\mu_{eg}$ increases as a result of a highly charge-separated ground state, μ_{eg} is diminished by the decrease in electronic connectivity between φ_a and φ_b, and E_{eg} is minimized (Figure 3A), consistent with the computed localization of HOMO and LUMO orbitals upon twisting (Figure 3B).

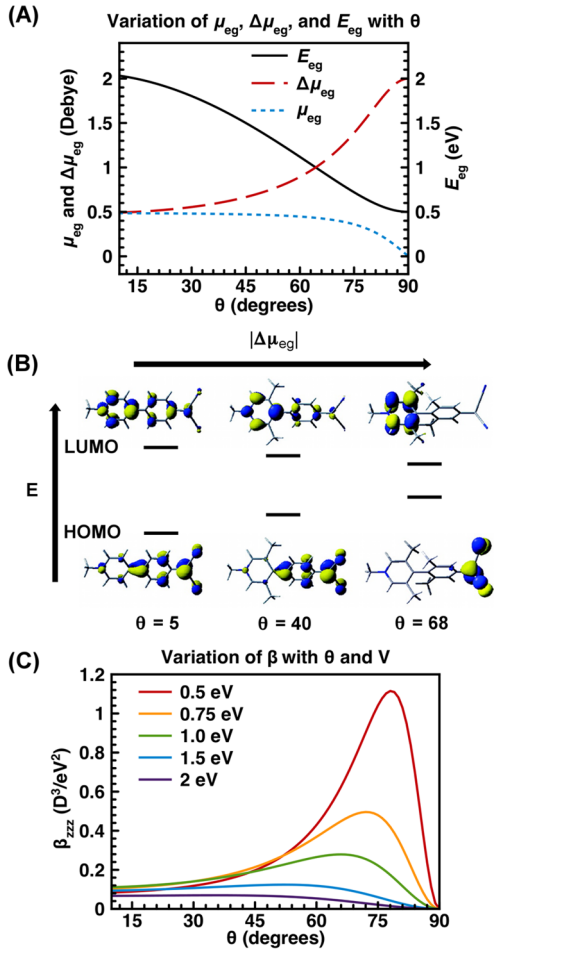

Figure 3. (A) Plots showing the dependence of $\Delta\mu_{eg}$, μ_{eg}, and E_{eg} derived from the 2-site Hückel model. V is set to 0.5 eV. (B) Representative correlation diagram with DFT derived orbitals. Adapted with permission from ref 20. Copyright 2008 American Chemical Society. (C) Dependence of β on θ for various values of V derived from eq 1.

Thus, the manipulation of θ can optimize parameters in eq 1 and enhance β (Figure 3C). The optimum value of θ is related to V, which is dictated by the donor and acceptor group identity. This simple model provides a convincing demonstration that for small values of V, massively enhanced β values occur at $\theta \approx 65-85°$. The intuitive reasoning here forms the basis for extensive investigations of TICT chromophore electronic structure and NLO response with a variety of quantum computational methods.[6,25−30] The pioneering computational studies (refs 23 and 24) explored the interplay

DOI: 10.1021/acs.accounts.9b00077
Acc. Chem. Res. 2019, 52, 1428−1438

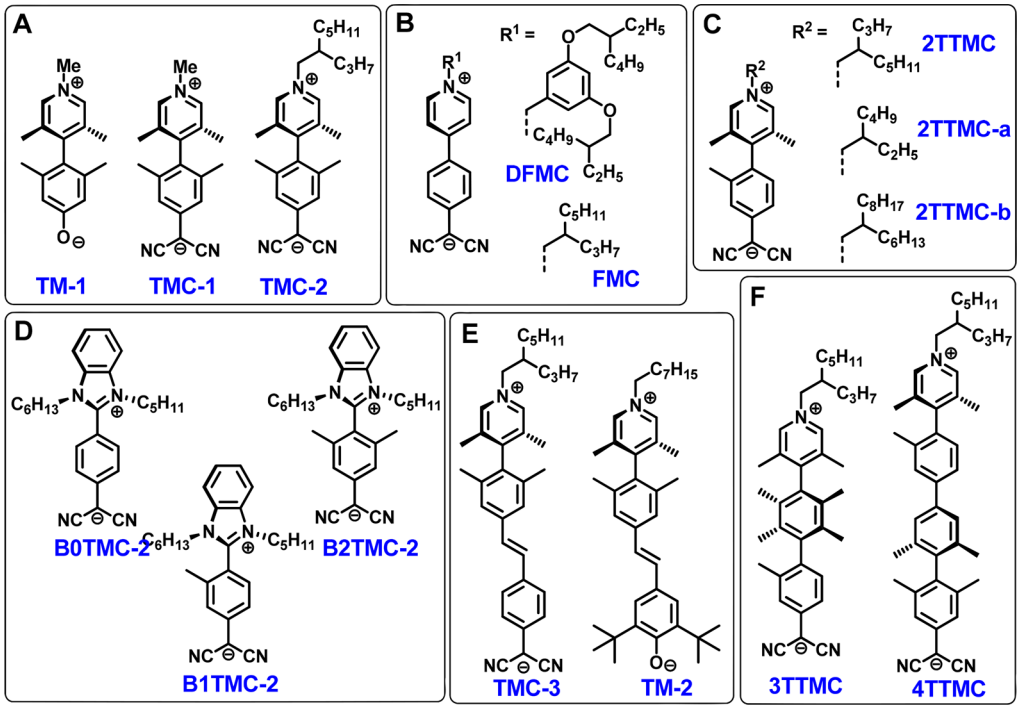

Figure 4. TICT chromophore structures, grouped by generation: (A) 1st generation chromophores, (B) planar analogues of **TMC-2**, (C) tri-*o*-methyl **TMC-2** derivatives, (D) benzimidazolium-based series, (E) extended conjugation structures, and (F) multiple twist.

Table 2. Selected Structural, Linear Optical, and Nonlinear Optical Properties of Second-Order TICT Chromophores[10,16−20]

					$\mu\beta$ ($\times10^{-48}$ esu)[c]	
chromophore	θ[a]	λ_{max} (nm)	ε (M^{-1} cm^{-1})	μ_g[f]	DCM	DMF
TMC-2[16,20]	89.6	569	1840	27.0[d] (29.8)[b]	−24 000	−5620
FMC[20]	9	582	63 900	14.1[b]	−4600	
DFMC[20]		585	62 100		−2360	
TMC-3[16]		540	2090	50.6[d]	−488 000	−84 000
TM-2[16]		462		37.3[d]	−315 000	−49 000
2TTMC[19]	78	560	1040	26.5[b]	−6000	
2TTMC-a[19]	85	561	5147	26.5[b]	−10 500	
2TTMC-b[19]		561	4164	26.5[b]	−10 600	
B0TMC-2[18]	64	434	24 930	21.2[e]	−10 300	−8400
B1TMC-2[18]	77	415	14 660	23.5[e]	−11 730	−12 740
B2TMC-2[18]	76	408	8160	24.6[e]	−26 000	−20 370

[a]Crystallographically derived, except for the last 3 entries. [b]INDO/S derived value. [c]Taken from lowest reliable concertation data point. [d]CASSCF derived value. [e]DFT derived value. [f]Note that μ_g does not vary greatly with computational method.

between θ and β, the influence of the dielectric environment and structural modifications, as well as the ground and excited state electronic structures; as such, they inform much of the chromophore design and experimental work discussed in this Account.

3.2. Impact of Molecular Structure Modification on Second-Order NLO Response

Measurements of TICT chromophores reported here (Figure 4, Table 2) were conducted by the DC electric field induced second harmonic generation (EFISH) method, which measures solution phase quantity $\mu\beta/5kT$, where μ is the computed ground state dipole moment, and $5kT$ accounts for thermal reorientation.[31] For these TICT chromophores, the quantity $\mu\beta$ is always negative, reflecting the fact that the $\mu_g > \mu_e$, such that $\Delta\mu_{eg} < 0$ (see eq 1). Note that because of chromophore aggregation (Section 4) the most dilute EFISH measurements are taken to approximate the monomeric value of β or $\mu\beta$, and are in many cases a lower bound on the magnitude of $\mu\beta$ because of experimental/instrumental constraints.[16,18]

3.3.1. Torsional Angle Effects. Wang et al.[20] compared tetra-*o*-methyl biaryl chromophore **TMC-2** (θ = ∼90°) to the more planar analogue **FMC** (θ = ∼9.0°), finding that **FMC** exhibits a higher ICT extinction coefficient (ε_{ICT}) of 63 900 M^{-1} cm^{-1} (ε_{ICT} = 1840 M^{-1} cm^{-1} for **TMC-2**) and a slight reduction in the ICT energy (Figure 5A). Relaxation of θ decreases μ_g by 15.7 D, which in turn reduces $\Delta\mu_{eg}$ from −21.4 D for **TMC-2** to −6.5 D for **FMC**, consistent with the smaller observed solvatochromic shift of the ICT peak. Even the slight reduction of θ from **TMC-2** (89.6°) to **2TTMC-b** (85.7°), as a result of *o*-methyl group deletion, increases ε_{ICT} to 4164 M^{-1} cm^{-1} in **2TTMC-b**, and both $\Delta\mu_{eg}$ and μ_g are computed to decrease by ∼2 D as compared to **TMC-2**.[19] EFISH measurements (Figure 5B) reveal that, for **TMC-2** type

DOI: 10.1021/acs.accounts.9b00077
Acc. Chem. Res. 2019, 52, 1428−1438

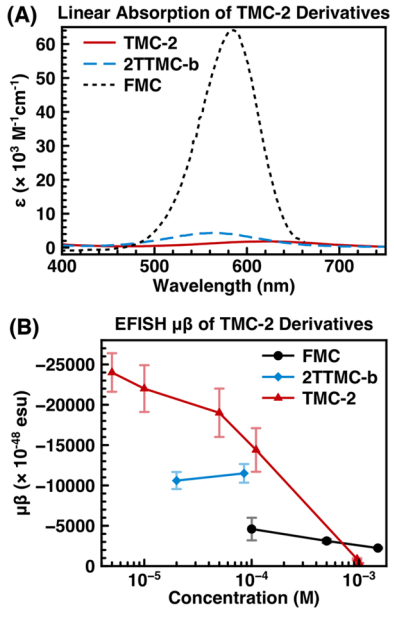

Figure 5. (A) Linear absorption of **TMC-2**, **2TTMC-b**, and **FMC** ICT peak in DCM solution. (B) EFISH results DCM solutions as a function of concentration.[16,19,20]

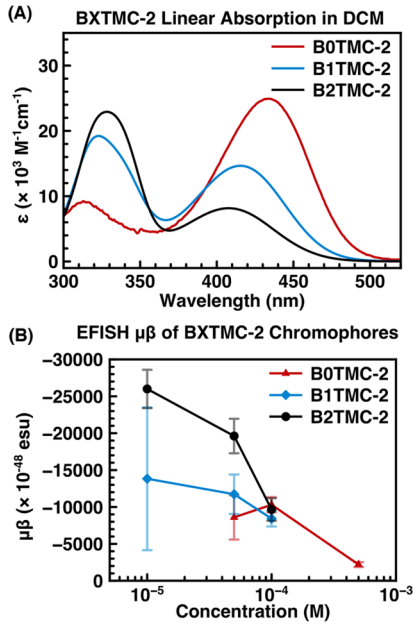

Figure 6. (A) Linear absorption of **BXTMC-2** chromophores in DCM solution showing the ICT transition and higher energy subfragment transition. (B) EFISH results in DCM solution.[18] Adapted with permission from ref 18. Copyright 2018 American Chemical Society.

structures, changes in θ result in a ~5× fall in $\mu\beta$ for **FMC** and a ~ 2× fall for **2TTMC-b** versus **TMC-2**. The corresponding β values fall in magnitude in the order **TMC-2** (-805×10^{-30} esu) > **2TTMC-b** (-433×10^{-30} esu) > **FMC** (-326×10^{-30} esu). Given the spectroscopic and computational evidence, this trend is attributed to the enhancement in charge separated character of the ground state as θ approaches 90°.

Lou et al.[18] synthesized a series of benzimidazolium based chromophores (Figure 4D, **BXTMC-2**) with zero, one, or two *o*-methyl groups leading to solution phase biaryl torsional angle (determined by Nuclear Overhauser Effect NMR and linear optical absorption) (Figure 6A) which increase in the order **B0TMC-2** (θ = 65°) < **B1TMC-2** < **B2TMC-2** (θ = 79°). EFISH measurements in DCM solution (Figure 6B) show that $\mu\beta$ increases in the same order **B0** < **B1** < **B2**, again as a result of molecular torsion enhancing charge separation, evidenced by the trend in computed μ_g.

3.2.2. Donor and Acceptor Group Impact on Electronic Structure and *μβ*. The choice of donor/acceptor moieties is dictated by their ability to stabilize negative/positive charge, resist chemical degradation, and to participate in the ZA and NQ resonance structures. In general, the donor moiety dominates the HOMO properties, and the acceptor dictates the LUMO, both of which become increasingly localized on the respective fragments upon twisting (Figure 7).

The earliest set of TICT NLO chromophores[10,16,17] (**TM-1**, **TM-2**) utilized a phenolate donor group, yielding a large $\mu\beta$ of $-315\,000 \times 10^{-48}$ esu in **TM-2**. Incorporation of a more chemically robust dicyanomethanide group serves to stabilize the negative charge and enhance $\mu\beta$, likely by maximizing charge separation in the ground state. This modification leads to a ~7 D increase in μ_g from **TM-1** to **TMC-2**, and a ~ 0.1 eV decrease in oxidation potential resulting in an expansion of the HOMO−LUMO gap (Figure 8). The same modification in **TM-2** leads to an increase of μ_g from 37.3 to 50.6 D, resulting in a record value of $\mu\beta = -488\,000 \times 10^{-48}$ esu for **TMC-3**.

Until recently, TICT chromophores exclusively employed pyridinium acceptor groups which are chemically robust and

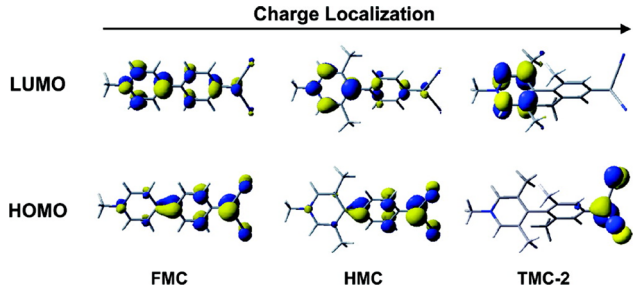

Figure 7. HOMO and LUMO localization upon twisting of **TMC-2** analogues **FMC** (θ = 5.1°), **HMC** (θ = 40.2°), and **TMC-2** (θ = 68°). Reproduced with permission from ref 20. Copyright 2008 American Chemical Society.

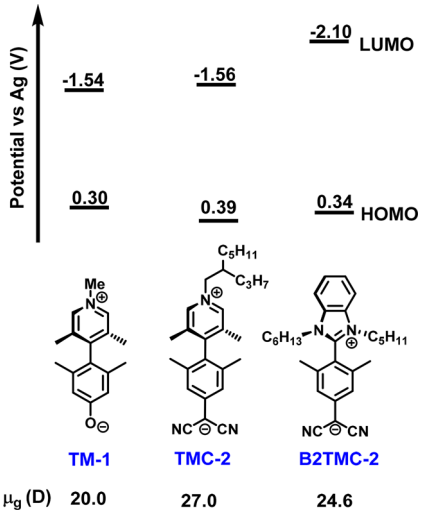

Figure 8. Electrochemical HOMO and LUMO levels vs Ag in ACN of chromophores **TM-1**, **TMC-2**, and **B2TMC-2**.

DOI: 10.1021/acs.accounts.9b00077
Acc. Chem. Res. 2019, 52, 1428−1438

allow for very large $\mu\beta$ values. Only recently, a benzimidazolium acceptor group was employed in the **BXTMC-2** series, raising the LUMO energy by ∼0.5 eV over the pyridinium analogue **TMC-2** (Figure 8).[18] The **BXTMC-2** μ_g values are reduced by ∼5 D due to a slight relaxation of θ and decreased spatial separation between the position of positive and negative charges. The NLO response of these chromophores is discussed in section 4.2.

3.3.3. Extended Conjugation. Kang et al.[16] extended the molecular conjugation length, thereby increasing the spatial separation between donor and acceptor moieties, thereby leading to large magnitudes of μ_g, $\Delta\mu_{eg}$, and $\mu\beta$.[16,18] Appending a stilbene fragment to the donor portion of archetypal chromophores **TMC-2** and **TM-1**, to create **TMC-3** and **TM-2** respectively, preserves the twisted fragment and maintains a largely charge separated ground state, as evidenced by the similar ε_{ICT} and λ_{ICT} in **TMC-2** and **TMC-3** (Figure 4E and Table 2). The ensuing 20× increase in $\mu\beta$ from **TMC-2** to **TMC-3** is attributed primarily to the increase in μ_g from 27.0 to 50.3 D. However, this strategy is limited by two factors: (1) increasing μ_g exacerbates a tendency for dipole-driven aggregate formation, limiting high $\mu\beta$ values to dilute solutions, and (2) decreasing the proximity of the donor group from the twisted C−C bond can reduce the benefit of aromatic stabilization, and therefore also erode the efficient ground-state charge separation, which contributes significantly to the NLO response.[25]

3.3.4. Multiple Twists in TICT Chromophores. In a recent study by Shi et al.,[19] chromophores with single (**2TTMC**), double (**3TTMC**), and triple (**4TTMC**) twists (Figure 4E) were synthesized in an effort to further enhance charge separation without introducing intricate and potentially unstable conjugated pathways. Quantum computation shows increasing HOMO and LUMO localization on the donor and acceptor fragments respectively with the addition of each twist (Figure 9), in agreement with the experimentally observed

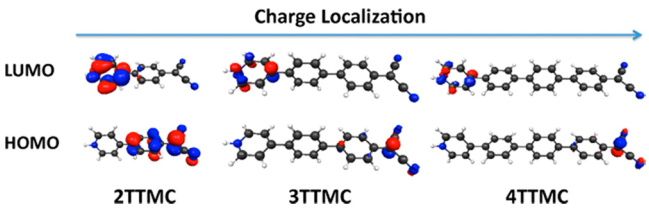

Figure 9. Isodensity surface plots of the HOMOs and LUMOs of the indicated TTMC chromophores computed at the B3LYP level with imposed twist angles. Note the increasing charge localization with enforced twist angle π-system extension. Reproduced with permission from ref 19. Copyright 2015 American Chemical Society.

enhanced basicity of the donor fragment in **3TTMC** and **4TTMC**. Spectroscopic and electrochemical measurements show that the addition of twisted fragments serves to (1) lower E_{eg}, as demonstrated by the decrease of electrochemically measured bandgap from 1.86 > 1.75 > 1.67 eV for **2TTMC**, **3TTMC**, **4TTMC** respectively, (2) increase μ_g to 74.0 D in **4TTMC**, and (3) reduce in ε_{ICT} (ε < 284 cm^{-1} M^{-1} for **4TTMC**) and, consequently, μ_{eg}, as the HOMO and LUMO become increasingly spatially separated.

Despite the large reduction in μ_{eg}, the changes in E_{eg} and μ_g can account for an impressive increase in $\mu\beta$, which is computed to be on the remarkable order of $-820\,000 \times 10^{-48}$ esu for **4TTMC** and $-327\,000 \times 10^{-48}$ esu for **3TTMC** (experimental verification was not possible). The key finding in the computational work is that only twisted biaryl junctions adjacent to the aromatic donor and acceptor moieties appreciably increase β, and that HOMO and LUMO localization is a key factor leading to linear scaling of β with the number of phenylene rings.

4. APPROACHES TO REDUCE TICT CHROMOPHORE AGGREGATION

As alluded to previously, large μ_g values also drive electrostatic, dipole−dipole-based attractive interactions, which cause TICT chromophores to form centrosymmetric aggregate structures in polymer matrices and in concentrated solutions, driving $\mu\beta$ to essentially zero. Thus, it has not been possible to realize the full potential of TICT chromophores in technologically relevant electro-optic devices, for which the target chromophore loading exceeds ∼5 wt %. For example, **TMC-3** (5 wt % in PVP) can exhibit a very large electro-optic coefficient of r_{33} ≈ 330 pm/V during poling, but upon removal of the poling field the restoration of dipole−dipole interactions renders r_{33} negligible.[16] Similarly, solution EFISH measurements of $\mu\beta$ fall significantly at higher chromophore concentrations as a direct result of the intermolecular interactions (Figure 10A).

The extent of these interactions can be quantified by the aggregation number (N), as derived from pulsed-gradient spin−echo (PGSE) NMR experiments (Figure 10B); these confirm the inverse relationship between aggregate formation and $\mu\beta$.[16,20] The interaction strength can be estimated by the crystallographic packing distances of antiparallel dimers (Figure 10C−E), as well as by the dimerization constants (K_d) determined by optical or NMR spectroscopy. **TMC-2** in DCM, exhibits a dimerization constant of K_d = 246 ± 30 M^{-1} and the Gibbs dimerization energy of ΔG_d^0 = −13.6 ± 0.3 kJ/mol which is similar in magnitude to that of a hydrogen bond.[16]

4.1. Side-Chain Modification Effects on TICT Aggregation

The introduction of bulky side chain substituents (R) on **TMC-1** derivatives can be used to suppress aggregation of the TICT chromophore π−systems (Table 3). For example, the R = 2-propylheptyl group in **TMC-2** causes a significant increase in the average crystallographic packing distance (Table 3) versus **TMC-1** (R = Me).[16] In the **2TTMC** series, increasing the R group size from 2-ethylhexyl to 2-propylheptyl reduces K_d, increases the crystallographic packing distance, and yields a slightly higher $\mu\beta$ at 10^{-4} M in DCM.[19] Larger R = 2-hexyldecyl substituents (**2TTMC-b**) increase K_d, likely reflecting stronger side chain-side chain interactions, although the concentration independence of $\mu\beta$ and the linear optical absorption data suggest that the type of aggregates present in **2TTMC-b** are not extremely detrimental to NLO response. For **TMC-2** type molecules, very large branched R groups encourage benign aggregates, which may even compete with formation of centrosymmetric ones. On the other hand, $\mu\beta$ decreases upon the introduction of a dendritic type R group (see Figure 1) to planar chromophore **FMC** (Figure 4C). The **FMC** series allows very close face-to-face antiparallel packing distances, which are ∼3 Å shorter[20] than those in **TMC-2**, reflecting a very strong propensity to aggregate.

4.2. Role of Chromophore Environment in Dictating Aggregation

The chromophore environment plays an important role in dictating aggregation tendencies. For example, in polar DMSO,

DOI: 10.1021/acs.accounts.9b00077
Acc. Chem. Res. 2019, 52, 1428−1438

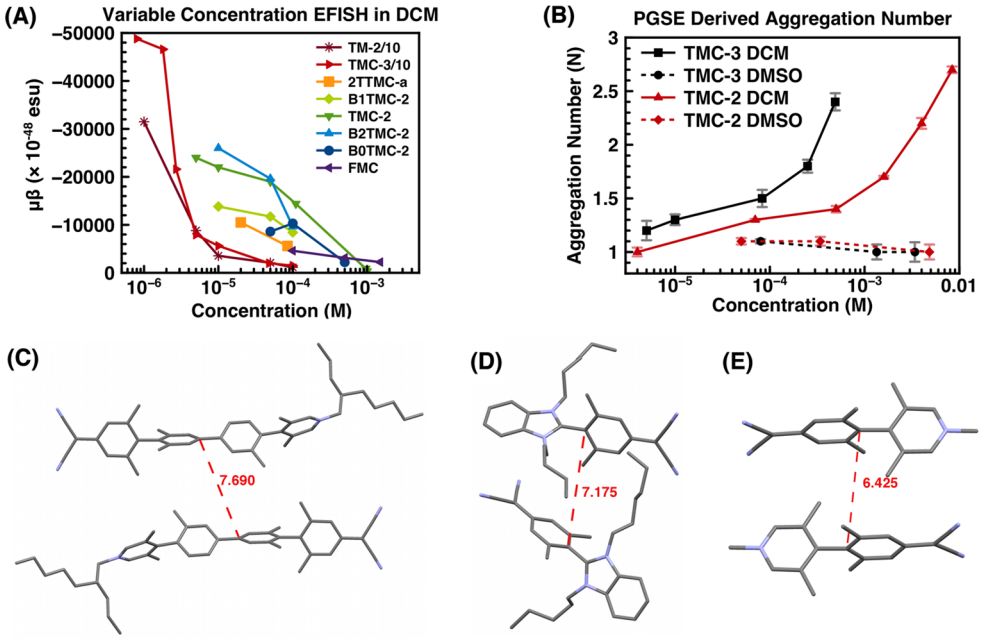

Figure 10. Aggregation of TICT chromophores and its influence on NLO response. (A) EFISH derived $\mu\beta$ of the indicated TICT chromophores as a function of concentrations in DCM solution; note the fall in $\mu\beta$ accompanying increased aggregation. (B) PGSE NMR derived aggregation numbers for **TMC-2** and **TMC-3** over a concentration range in DCM and DMSO solutions. Adapted with permission from ref 16. Copyright 2007 American Chemical Society. (C–E) Antiparallel aligned dimer units responsible for decrease in NLO response; shown here are the crystal structures of **4TTMC** (C), **B2TMC-2** (D), and **TMC-1** (E) with the closest intermolecular contacts given in Å.[16,19]

Table 3. Effect of Side Chain Modification on Crystal Structure Packing Distance between Antiparallel Pairs, Dimerization Constants (K_d), and $\mu\beta$ Values in Concentrated Solutions

			K_d (M^{-1})[b]		~10^{-4} M in CH_2Cl_2	
chromophore	R substituent	packing distance (Å)[a]	$CHCl_3$	CH_2Cl_2	N[c]	$\mu\beta$ ($\times 10^{-48}$ esu)
TMC-1[16]	methyl	7.418				
TMC-2[16]	2-propylheptyl	8.128	13 300 ± 1420	141 ± 62	1.00	−14 400
2TTMC[19]	2-propylheptyl	8.601	6700 ± 400			−6000
2TTMC-a[19]	2-ethylhexyl	8.387	12 200 ± 300			−5600
2TTMC-b[19]	2-hexyldecyl		28 300 ± 300			−11 500
FMC[20]	2-propylheptyl	5.160		215 ± 24	1.06	−4600
DFMC[20]	dendritic			264 ± 47	1.03	−2350

[a]Packing distance measured as the distance between the bridging carbon on the pyridinium ring of the closest packed antiparallel pair. [b]K_d derived from NMR experiments in $CHCl_3$ and CH_2Cl_2. [c]Aggregation number derived from PGSE NMR experiments.

both **TMC-2** and **TMC-3** exist as monomers at concentrations as high as ~3 mM (Figure 10). Unfortunately, polar solvents also stabilize the electronic ground state and increase E_{eg}, which significantly diminishes $\mu\beta$ (Figure 11).[6] Recently, the use of a benzimidazolium acceptor group has remedied this issue by increasing the stability of the cationic portion such that E_{eg} is comparable in DCM and DMF solutions; the **BXTMC-2** series (Figure 4D) exhibits $\mu\beta$ as high as 20,370 × 10^{-48} esu for **B2TMC-2** in polar DMF, and the reduced aggregation extends the excellent NLO response to unprecedently high concentrations of ~1 mM (Figure 11).[18]

Another approach by Lou et al.[32] uses nonvolatile salts to introduce ionic interactions that compete with **B2TMC-2** self-aggregation. The addition of small amounts of tetra-*n*-butylphosphonium bromide ($Bu_4P^+Br^-$) to highly aggregated solutions of **B2TMC-2** in $CHCl_3$ results in halochromic shifts in the λ_{ICT}, indicating that $Bu_4P^+Br^-$ interacts strongly with **B2TMC-2**, primarily through attraction between the Br^- anion and the chromophore cationic terminus (Figure 12A). EFISH measurements in solutions with varied $Bu_4P^+Br^-$ and **B2TMC-**

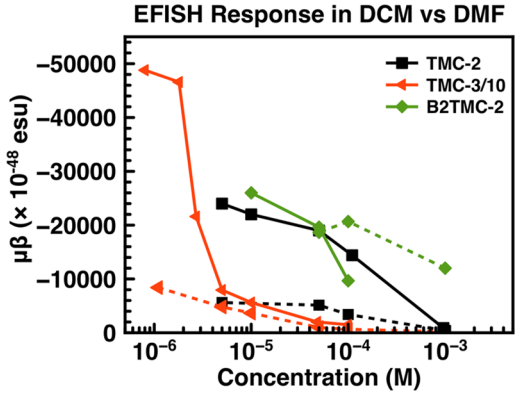

Figure 11. Comparison of EFISH derived $\mu\beta$ of chromophores **TMC-2**, **TMC-3**, and **B2TMC-2** in DCM (solid lines) and polar DMF solutions (dotted lines) as a function of concentration. Both **TMC-3** data sets are scaled by 10^{-1} for clarity.[16,18]

DOI: 10.1021/acs.accounts.9b00077
Acc. Chem. Res. 2019, 52, 1428–1438

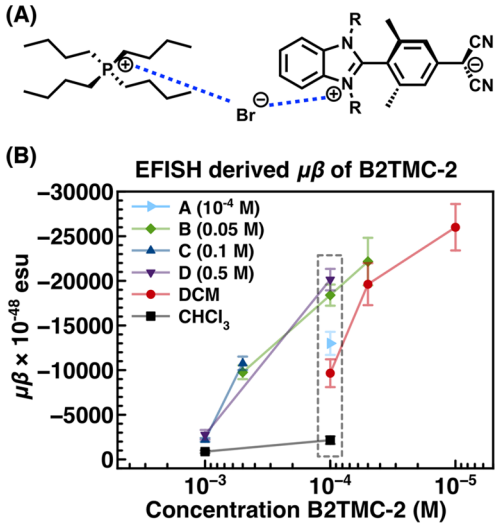

Figure 12. (A) Proposed interaction between chromophore **B2TMC-2** and added $Bu_4P^+Br^-$. (B) EFISH derived $\mu\beta$ of **B2TMC-2** in DCM solution and $CHCl_3$ solutions with varied concentrations of added $Bu_4P^+Br^-$(as noted in the legend). The dotted box is intended to facilitate the comparison for 10^{-4} M **B2TMC-2** solutions. Reproduced with permission from ref 32. Copyright 2018 Wiley.

2 concentration reveal a shift in the onset of aggregate formation which extends the region of high $\mu\beta$ to higher concentrations (Figure 12B). Similar changes in optical absorption were observed in PMMA/**B2TMC-2**/$Bu_4P^+Br^-$ films, suggesting that the same beneficial interactions also persist in the film; E-O measurements on such films are ongoing.

4.3. Toward Bulk E-O Materials

Ultimately, the best metric for the utility of the TICT chromophores is the product of number density, approximated here by concentration, M, and $\mu\beta$, denoted here as "$N\mu\beta$".[9] Figure 13 shows that by balancing attributes that produce large $\mu\beta$ with those properties or conditions which reduce aggregation, the maximum in $N\mu\beta$ can be manipulated by nearly 3 orders of magnitude in concentration toward the target value of ∼0.1 M. From this analysis, it can be seen that **B2TMC-2** is a promising candidate, particularly in combination with the approach described in section 4.2.

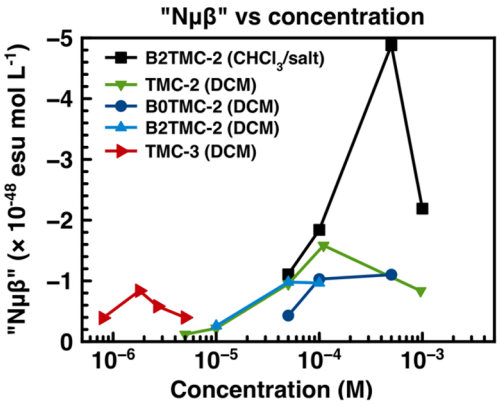

Figure 13. Concentration dependence of $N\mu\beta$ for selected TICT chromophores in the indicated solvents. Only data over a meaningful concentration range are plotted, and lines are drawn as a guide to the eye.

5. THIRD-ORDER NONLINEAR OPTICAL RESPONSE

The third-order NLO response takes the form of nonlinear refraction and absorption, which are denoted by molecular quantities $Re(\gamma)$ and $Im(\gamma)$, respectively. Z-scan measurement of **TMC-2** (at 800 nm in CH_2Cl_2) by He et al.[13] reveals $Re(\gamma) = 1.4 \times 10^{-33}$ esu and $Im(\gamma) = 3.43 \times 10^{-35}$ esu, giving a $Re(\gamma)/Im(\gamma) \gg 12$, which is considered to be the minimum value for all-optical signal processing (AOSP) applications.[33] Assuming that only one low-lying state is strongly coupled to the ground state, a truncated three-level sum-over-states model (eq 2) for off-resonant γ can be employed to guide molecular design.[34] Here, γ is defined

$$\gamma = -\frac{\mu_{eg}^{4}}{E_{eg}^{3}} + \frac{\mu_{eg}^{2}\Delta\mu_{eg}^{2}}{E_{eg}^{3}} + \frac{\mu_{eg}^{2}\mu_{e,e}^{2}}{E_{eg}^{2}E_{e,g}} \qquad (2)$$

by three terms, which are composed of the transition energies, transition moments, and state dipole moments of the electronic ground and excited states (e and e′). As the second (dipolar) term appears to dominate $Re(\gamma)$, TICT chromophores (Figure 14, Table 4) do not depend on strongly absorbing transitions that can contribute to linear and nonlinear loss.

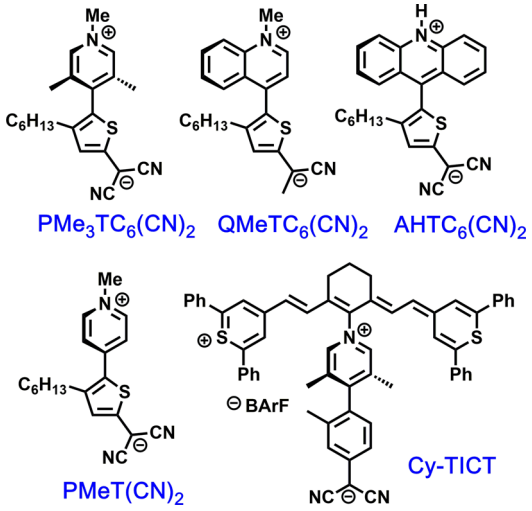

Figure 14. TICT chromophores for third-order NLO applications.

As with β, the chromophore ground-state charge separation is a key factor relating γ to modifications in θ and the donor and acceptor moieties. Close energetic spacing of the ground and ICT state, as well as the presence of a twisted bridging orbital are also key factors dictating NLO response.[13] The special properties of biradical systems, as described by Nakano et al.,[35−38] may also contribute to the current understanding, and this is a field of active exploration. Note that unlike with β, the introduction of an aggregate-based center of symmetry does not necessarily compromise γ. However, concentration-dependent studies have proven instrumentally challenging, so our understanding of aggregation effects and other loss mechanisms such as scattering is currently incomplete.

5.1. Thiophene Based TICT Chromophores

Teran et al.[15] synthesized a series of **TMC-2** derivatives in which the donor aryl group is replaced by an election rich thiophene (Figure 14). **$PMe_3TC_6(CN)_2$**, the direct analogue of **TMC-2**, exhibits a ∼0.5 eV rise in HOMO energy reflecting

DOI: 10.1021/acs.accounts.9b00077
Acc. Chem. Res. 2019, 52, 1428−1438

Table 4. *Z*-Scan-Derived *Re* and *Im* Parts of γ in Selected Solvents and at the Indicated Wavelengths (nm)[13−15]

		$Re(\gamma)$ ($\times 10^{-33}$ esu)				$Im(\gamma)$ ($\times 10^{-35}$ esu)			
chromophore	solvent	800	1100	1300	1400	800	1100	1300	1400
TMC-2[13]	DCM	1.4	0.5			3.43	<1.3		
$PMe_3TC_6(CN)_2$[15]	DCM	−14.2				<1.63			
	ACN	0.24	<0.12			<1.63	<1.63		
$QMeTC_6(CN)_2$[15]	BzOH	0.50		<0.24		<1.63		<1.63	
Cy-TICT[14]	DCM			−6.43	−2.27			58.8	15.8
	ACN			−3.50				10.8	

the fall in aromatic stabilization engendered by the thiophene moiety, and subsequently a lower E_{01} energy gap. The increased electron density of the donor fragment also enhances the degree of ground state charge separation (μ_g = 35.4 D), and a slight relaxation of θ serves to increase μ_{ge} to ∼5 D by allowing better HOMO−LUMO overlap (Figure 15B). The

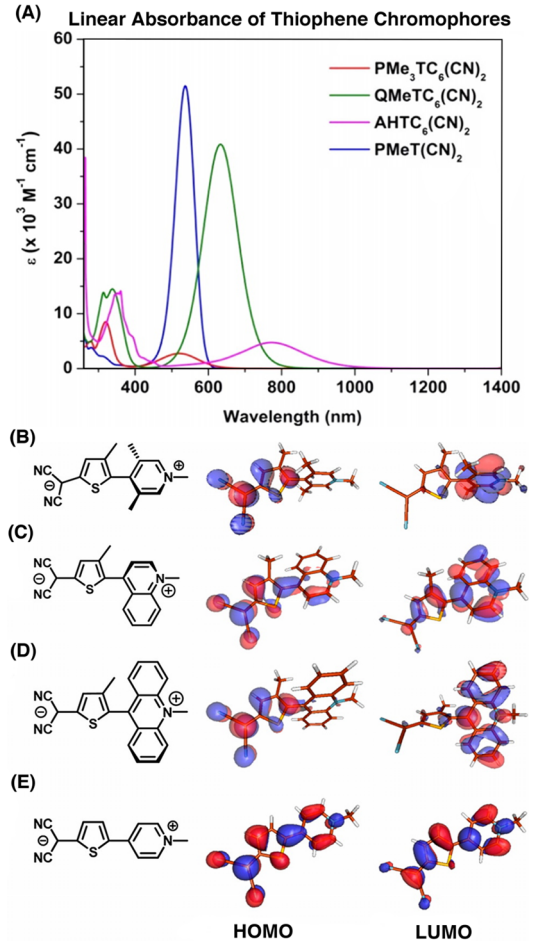

Figure 15. (A) Linear absorbance of thiophene chromophores in DCM. (B−E) HOMO and LUMO isodensity plots for structural equivalents of (B) **$PMe_3TC_6(CN)_2$**, (C) **$QMeTC_6(CN)_2$**, (D) **$AHTC_6(CN)_2$**, and (E) **$PMeT(CN)_2$**. Adapted with permission from ref 15. Copyright 2016 American Chemical Society.

combination of these factors results in remarkably large Re(γ) = -14.2×10^{-33} esu for **$PMe_3TC_6(CN)$** in DCM at 800 nm, in agreement with the expected trend from eq 2. The nonlinear absorption remains low, with $Im(\gamma) < 1.63 \times 10^{-35}$ esu.

The relationship between θ and Re(γ) was probed using the planar analogue, **$PMeT(CN)_2$**, which exhibits significantly stronger absorption because of a high degree of HOMO−LUMO overlap (Figure 15E), a 0.2 eV increase in the HOMO−LUMO gap, and a decrease in μ_g to 21.0 D. The relaxed biaryl torsion also removes the manifold of low-lying excited states (beyond the first ICT transition) found in **$PMe_3TC_6(CN)_2$** which can contribute to γ. These factors cause a two order-of-magnitude decrease in $Re(\gamma)$ from **$PMe_3TC_6(CN)_2$** ($\theta \approx 75°$) to **$PMeT(CN)_2$** ($\theta = 0°$) as computed at 1550 nm in $CHCl_3$.

Annelating arene rings onto the pyridinium acceptor to form quinoline (**$QMeTC_6(CN)_2$**) and acridine (**$AHTC_6(CN)_2$**) based chromophores (Figure 14) primarily impacts the LUMO characteristics, although the concurrent changes in steric constraints also relax θ and lead to delocalization of both HOMO and LUMO orbitals (Figure 15B−D). LUMO delocalization across progressively larger π-systems in **$QMeTC_6(CN)_2$** and **$AHTC_6(CN)_2$** provides energetic stabilization, compressing the HOMO−LUMO gap, as seen by shifts in λ_{ICT} (Figure 15A), and aromatic stabilization from the auxiliary rings causes **$AHTC_6(CN)_2$** to exhibit significant NQ character. Compared to **$PMe_3TC_6(CN)$**, **$QMeTC_6(CN)_2$** exhibits relaxed torsion ($\theta \sim 40°$), leading to increased μ_{ge} = 10 D, and slightly decreased μ_g = 32.1 D. However, because of the HOMO and LUMO delocalization, $\Delta\mu_{eg}$ decreases relative to **$PMe_3TC_6(CN)$**, and **$QMeTC_6(CN)_2$** exhibits a modest $Re(\gamma) = 0.5 \times 10^{-33}$ esu.

5.2. Cyanine/TICT Hybrids

Shi et al.[14] investigated the impact of coupling TICT chromophore **2TTMC** to a cyanine dye, **IR-1061** ($Re(\gamma) = -3.78 \times 10^{-33}$ esu at 1305 nm). Linear optical absorption spectra (Figure 16A) of the hybrid **Cy-TICT** chromophore reveals a broadening and weakening of the principle transition in **IR-1061** from μ_{eg} of 18.7 to 12.1 D, and a large negative solvatochromic shift typical of TICT chromophores. Both changes are consistent with a truly hybridized system. This character is further evidenced by the MO descriptions of the frontier orbitals (Figure 16B), which reveals both the TICT and cyanine character of **Cy-TICT**. Cross-coupling between the closely spaced twisted chromophore and cyanine states leads to a cooperatively enhanced $Re(\gamma)$ value of -6.43×10^{-33} esu at 1305 nm.

6. CONCLUSIONS

TICT chromophores are very promising candidates for NLO applications ranging from electro-optics to optical switching. Diverse classes of TICT chromophores have been developed to explore the impact of various structural modifications. While the third-order materials are still the subject of fundamental curiosity, the second-order chromophores are reaching sufficient maturity where demonstrations of large nonlinearities in dilute solution must be accompanied by implementation in

DOI: 10.1021/acs.accounts.9b00077
Acc. Chem. Res. 2019, 52, 1428−1438

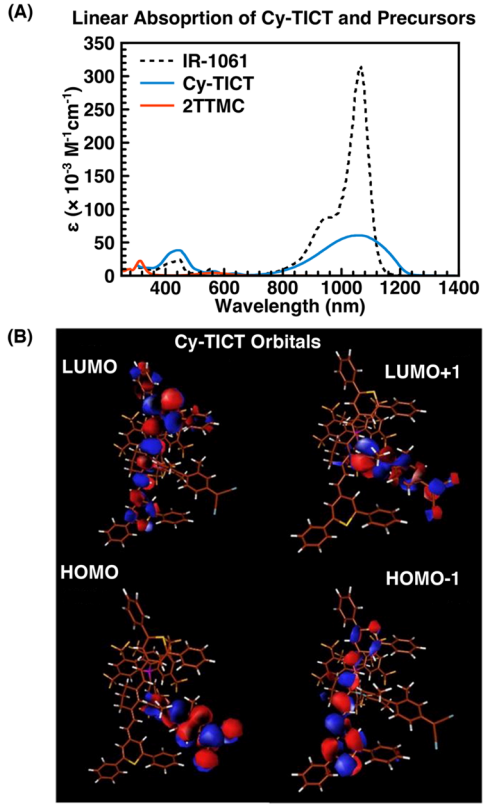

Figure 16. (A) Linear optical absorbance in DCM of the parent TICT (**2TTMC**) and cyanine (**IR-1061**) chromophores and hybrid chromophore **Cy-TICT**. (B) Isodensity plot of the **Cy-TICT** frontier orbitals; note that each orbital has distinct characteristics of the parent chromophores.[14] Adapted with permission from ref 14. Copyright 2015 American Chemical Society.

realistic films for prototype devices. That will require intense investigation into strategies to mitigate molecule aggregation and environmental effects while maximizing NLO metrics. The first steps have already been taken in recent publications, involving both chemical modification of the chromophores themselves and their environment. Achieving this goal should produce materials in which the electro-optic coefficients far exceed those of current commercial materials, and the robust nature of these molecules suggests that they have great potential as E-O candidates.

AUTHOR INFORMATION

Corresponding Author

*E-mail: t-marks@northwestern.edu.

ORCID

Tobin J. Marks: 0000-0001-8771-0141

Funding

AFOSR MURI grant F9550-14-1-0040.

Notes

The authors declare no competing financial interest.

Biographies

Alexander J.-T. Lou was born in Niskayuna, New York. He received a B.A. with Honors from Williams College and Ph.D. in Chemistry from Northwestern University in 2018, where he was a National Defense Science and Engineering Graduate Fellow. He is currently a Research Scientist at Nanosyn, Inc.

Tobin J. Marks was born in Washington, D.C. He is currently Ipatieff Professor of Chemistry and Professor of Materials Science and Engineering at Northwestern University. He received a B.S. degree from the University of Maryland and a Ph.D. from MIT in Chemistry. He is a member of the U.S. National Academy of Sciences, a Fellow of the American Academy of Arts and Sciences, a Member of the German, Italian, and Indian Academies of Sciences, and a Fellow of the Royal Society of Chemistry. Among other recognitions, he received the U.S. National Medal of Science and the American Chemical Society Priestly Medal.

ACKNOWLEDGMENTS

We would like to acknowledge our collaborators for their stimulating contributions to this effort: Dr. Alexander Baev, Prof. Elena Cariati, Prof. Antonio Facchetti, Dr. Guang He, Prof. Alceo Macchioni, Prof. Paras Prasad, and Prof. Cristiano Zuccacia.

ABBREVIATIONS

NLO, nonlinear optics; TICT, twisted intramolecular charge transfer; E-O, electro-optic; ICT, interfragment charge transfer

REFERENCES

(1) Zhan, C.; Yao, J. More than Conformational "Twisting" or "Coplanarity": Molecular Strategies for Designing High-Efficiency Nonfullerene Organic Solar Cells. *Chem. Mater.* **2016**, *28*, 1948−1964.

(2) Tao, Y.; Yuan, K.; Chen, T.; Xu, P.; Li, H.; Chen, R.; Zheng, C.; Zhang, L.; Huang, W. Thermally Activated Delayed Fluorescence Materials Towards the Breakthrough of Organoelectronics. *Adv. Mater.* **2014**, *26*, 7931−7958.

(3) Zhang, Q.; Li, J.; Shizu, K.; Huang, S.; Hirata, S.; Miyazaki, H.; Adachi, C. Design of Efficient Thermally Activated Delayed Fluorescence Materials for Pure Blue Organic Light Emitting Diodes. *J. Am. Chem. Soc.* **2012**, *134*, 14706−14709.

(4) Sasaki, S.; Drummen, G. P. C.; Konishi, G.-i. Recent Advances in Twisted Intramolecuar Charge Transfer (TICT) Fluorescence and Related Phenomena in Materials Chemisty. *J. Mater. Chem. C* **2016**, *4*, 2731−2743.

(5) Grabowski, Z. R.; Rotkiewicz, K.; Rettig, W. Structural Changes Accompanying Intramolecular Electron Transfer: Focus on Twisted Intramolecular Charge-Transfer States and Structures. *Chem. Rev.* **2003**, *103*, 3899−4031.

(6) Brown, E. C.; Marks, T. J.; Ratner, M. A. Nonlinear Response Properties of Ultralarge Hyperpolarizability Twisted π-System Donor-Acceptor Chromophores. Dramatic Environmental Effects on Response. *J. Phys. Chem. B* **2008**, *112*, 44−50.

(7) Chen, A.; Murphy, E. *Broadband Optical Modulators: Science, Technology, and Applications*; Taylor & Francis: New York, NY, 2011.

(8) Dalton, L.; Gunter, P.; Jazbinsek, M.; Kwon, O.-P.; Sullivan, P. *Organic Electro-optics and Photonics*; Cambridge University Press: Cambridge, UK, 2015; pp 1−293.

(9) Benight, S. J.; Bale, D. H.; Olbricht, B. C.; Dalton, L. R. Organic Electro-Optics: Understanding Material Structure/Function Relationships and Device Fabrication Issues. *J. Mater. Chem.* **2009**, *19*, 7466−7475.

(10) Kang, H.; Facchetti, A.; Zhu, P.; Jiang, H.; Yang, Y.; Cariati, E.; Righetto, S.; Ugo, R.; Zuccaccia, C.; Macchioni, A.; Stern, C. L.; Liu, Z.; Ho, S. T.; Marks, T. J. Exceptional Molecular Hyperpolarizabilities in Twisted pi-Electron System Chromophores. *Angew. Chem., Int. Ed.* **2005**, *44*, 7922−7925.

(11) Cho, M. J.; Choi, D. H.; Sullivan, P. A.; Akelaitis, A. J. P.; Dalton, L. R. Recent Progress in Second-Order Nonlinear Optical Polymers and Dendrimers. *Prog. Polym. Sci.* **2008**, *33*, 1013−1058.

DOI: 10.1021/acs.accounts.9b00077
Acc. Chem. Res. 2019, 52, 1428−1438

(12) Sun, S.-S.; Dalton, L. R. *Introduction to Organic Electronic and Optoelectronic Materials and Devices*; Taylor & Francis: New York, 2008.
(13) He, G. S.; Zhu, J.; Baev, A.; Samoć, M.; Frattarelli, D. L.; Watanabe, N.; Facchetti, A.; Ågren, H.; Marks, T. J.; Prasad, P. N. Twisted π-System Chromophores: Novel Pathway to All-Optical Switching. *J. Am. Chem. Soc.* **2011**, *133*, 6675−6680.
(14) Shi, Y.; Lou, A. J.-T.; He, G. S.; Baev, A.; Swihart, M. T.; Prasad, P. N.; Marks, T. J. Cooperative Coupling of Cyanine and Tictoid Twisted π-Systems to Amplify Organic Chromophore Cubic Nonlinearities. *J. Am. Chem. Soc.* **2015**, *137*, 4622−4625.
(15) Teran, N. B.; He, G. S.; Baev, A.; Shi, Y.; Swihart, M. T.; Prasad, P. N.; Marks, T. J.; Reynolds, J. R. Twisted Thiophene-Based Chromophores with Enhanced Intramolecular Charge Transfer for Cooperative Amplification of Third-Order Optical Nonlinearity. *J. Am. Chem. Soc.* **2016**, *138*, 6975−6984.
(16) Kang, H.; Facchetti, A.; Jiang, H.; Cariati, E.; Righetto, S.; Ugo, R.; Zuccaccia, C.; Macchioni, A.; Stern, C. L.; Marks, T. J.; et al. Ultra-large Hyperpolarizability Twisted π-Electron System Electro-optic Chromophores. *J. Am. Chem. Soc.* **2007**, *129*, 3267−3286.
(17) Kang, H.; Facchetti, A.; Stern, C. L.; Rheingold, W. S.; Marks, T. J.; et al. Efficient Synthesis and Structural Characteristics of Zwitterionic Twisted π-Electron System Biaryls. *Org. Lett.* **2005**, *7*, 3721.
(18) Lou, A. J.-T.; Righetto, S.; Barger, C.; Zuccaccia, C.; Cariati, E.; Macchioni, A.; Marks, T. J. Unprecedented Large Hyperpolarizability of Twisted Chromophores in Polar Media. *J. Am. Chem. Soc.* **2018**, *140*, 8746−8755.
(19) Shi, Y.; Frattarelli, D.; Watanabe, N.; Facchetti, A.; Cariati, E.; Righetto, S.; Tordin, E.; Zuccaccia, C.; Macchioni, A.; Wegener, S. L.; Stern, C. L.; Ratner, M. A.; Marks, T. J. Ultra-High-Response, Multiply Twisted Electro-optic Chromophores: Influence of π-System Elongation and Interplanar Torsion on Hyperpolarizability. *J. Am. Chem. Soc.* **2015**, *137*, 12521−12538.
(20) Wang, Y.; Frattarelli, D. L.; Facchetti, A.; Cariati, E.; Tordin, E.; Ugo, R.; Zuccaccia, C.; Macchioni, A.; Wegener, S. L.; Stern, C. L.; Ratner, M. A.; Marks, T. J. Twisted π-Electron System Electrooptic Chromophores. Structural and Electronic Consequences of Relaxing Twist-Inducing Nonbonded Repulsions. *J. Phys. Chem. C* **2008**, *112*, 8005−8015.
(21) Kuzyk, M. G.; Singer, K. D.; Stegeman, G. I. Theory of Molecular Nonlinear Optics. *Adv. Opt. Photonics* **2013**, *5*, 4−82.
(22) Kuzyk, M. G.; Perez-Moreno, J.; Shafei, S. Sum Rules and Scaling in Nonlinear Optics. *Phys. Rep.* **2013**, *529*, 297−398.
(23) Perez-Moreno, J.; Zhao, Y.; Clays, K.; Kuzyk, M. G. Modulated Conjugation as a Means for Attaining a Record High Intrinsic Hyperpolarizability. *Opt. Lett.* **2007**, *32*, 59−61.
(24) Lytel, R.; Mossman, S. M.; Kuzyk, M. G. Phase Disruption as a New Design Paradigm for Optimizing the Nonlinear-Optical Response. *Opt. Lett.* **2015**, *40*, 4735−4738.
(25) Albert, I. D. L.; Marks, T. J.; Ratner, M. A. Remarkable NLO Response and Infrared Absorption in Simple Twisted Molecular π-Chromophores. *J. Am. Chem. Soc.* **1998**, *120*, 11174−11181.
(26) Albert, I. D. L.; Marks, T. J.; Ratner, M. A. Conformationally-Induced Geometric Electron Localization. Interrupted Conjugation, Very Large Hyperpolarizabilities, and Sizable Infrared Absorption in Simple Twisted Molecular Chromophores. *J. Am. Chem. Soc.* **1997**, *119*, 3155−3156.
(27) Pati, S. K.; Marks, T. J.; Ratner, M. A. Conformationally Tuned Large Two-Photon Absorption Cross Section in Simple Molecular Chromophores. *J. Am. Chem. Soc.* **2001**, *123*, 7287−7291.
(28) Keinan, S.; Zojer, E.; Brédas, J.-L.; Ratner, M. A.; Marks, T. J. Twisted π-system electro-optic chromophores. A CIS vs. MRD-CI theoretical investigation. *J. Mol. Struct.: THEOCHEM* **2003**, *633*, 227−235.
(29) Isborn, C. M.; Davidson, E. R.; Robinson, B. H. Ab Initio Diradical/Zwitterionic Polarizabilities and Hyperpolarizabilities in Twisted Double Bonds. *J. Phys. Chem. A* **2006**, *110*, 7189−7196.
(30) Albert, I. D. L.; Marks, T. J.; Ratner, M. A. Rational Design of Molecules with Large Hyperpolarizabilities. Electric Field, Solvent Polarity, and Bond Length Alternation Effects on Merocyanine Dye Linear and Nonlinear Optical Properties. *J. Phys. Chem.* **1996**, *100*, 9714−9725.
(31) Prasad, P. N.; Williams, D. J. *Introduction to Nonlinear Optical Effects in Molecules and Polymers*; John Wiley & Sons: New York, 1991.
(32) Lou, A. J.-T.; Righetto, S.; Cariati, E.; Marks, T. J. Organic Salts Suppress Aggregation and Enhance the Hyperpolarizability of a pi-Twisted Chromophore. *Chem. - Eur. J.* **2018**, *24*, 15801−15805.
(33) Hales, J. M.; Matichak, J. D.; Barlow, S.; Ohira, S.; Yesudas, K.; Bredas, J. L.; Perry, J. W.; Marder, S. R. Design of Polymethine Dyes with Large Third-Order Optical Nonlinearities and Loss Figures of Merit. *Science* **2010**, *327*, 1485−1487.
(34) Meyers, F.; Marder, S. R.; Pierce, B. M.; Bredas, J. L. Tuning of Large Second Hyperpolarizabilities in Organic Conjugated Compounds. *Chem. Phys. Lett.* **1994**, *228*, 171−176.
(35) Nakano, M.; Minami, T.; Fukui, H.; Yoneda, K.; Shigeta, Y.; Kishi, R.; Champagne, B.; Botek, E. Approximate Spi-Projected Spin-Unrestricted Density Functional Theory Method: Application to the Diradical Character Dependences of the (Hyper)polarizabilities in p-quinodimethane Models. *Chem. Phys. Lett.* **2010**, *501*, 140.
(36) Nakano, M.; Champagne, B.; Botek, E.; Ohta, K.; Kamada, K.; Kubo, T. Giant Electric Field Effect on the Second Hyperpolarizability of Symmetric Singlet Diradical Molecules. *J. Chem. Phys.* **2010**, *133*, 154302.
(37) Nakano, M.; Champagne, B. Diradical Character Dependences of the First and Second Hyperpolarizabilities of Asymmetric Open-Shell Singlet Systems. *J. Chem. Phys.* **2013**, *138*, 244306.
(38) Nakano, M.; Champagne, B. Theoretical Design of Open-Shell Singlet Molecular Systems for Nonlinear Optics. *J. Phys. Chem. Lett.* **2015**, *6*, 3236−3256.

DOI: 10.1021/acs.accounts.9b00077
Acc. Chem. Res. 2019, 52, 1428−1438